

# A Hominid from the Lower Pleistocene of Atapuerca, Spain: Possible Ancestor to Neandertals and Modern Humans

J. M. Bermúdez de Castro\*, J. L. Arsuaga, E. Carbonell, A. Rosas, I. Martínez, M. Mosquera

Human fossil remains recovered from the TD6 level (Aurora stratum) of the lower Pleistocene cave site of Gran Dolina, Sierra de Atapuerca, Spain, exhibit a unique combination of cranial, mandibular, and dental traits and are suggested as a new species of *Homo*—*H. antecessor* sp. nov. The fully modern midfacial morphology of the fossils antedates other evidence of this feature by about 650,000 years. The midfacial and subnasal morphology of modern humans may be a retention of a juvenile pattern that was not yet present in *H. ergaster*. *Homo antecessor* may represent the last common ancestor for Neandertals and modern humans.

Even though there is general agreement about the existence of an evolutionary continuity between the European middle Pleistocene hominids and the Neandertals, the origin of this lineage remains under discussion. Traditionally, the European middle Pleistocene fossils have been considered to be early representatives of *Homo sapiens* that were transitional between *H. erectus* and modern humans (1). More recently, they have been interpreted, together with some African specimens of similar chronology, as representatives of the stem species (*H. heidelbergensis*) of Neandertals and *H. sapiens* (2). However, the variation observed in the Afro-European hypodigm raises doubts about the validity of this model. From 1994 to 1996 nearly 80 human fossil remains have been recovered from level six (Aurora stratum) of the Pleistocene cave site of Gran Dolina (TD), Sierra de Atapuerca, Burgos, Spain (3). These hominids, which were found in sediments located about 1 m below the Matuyama-Brunhes boundary (4), shed light on the origin of both the European middle Pleistocene population and *H. sapiens*. Here we describe the TD6 fossils and suggest that these may represent a new species of *Homo*, which we name *Homo antecessor* sp. nov. [see (5); Table 1] to accommodate the variability observed in these hominids.

The TD6 human hypodigm includes numerous postcranial remains representing different skeletal parts, as well as some neurocranial, mandibular, facial, and dental specimens [Tables 2 and 3 and table 1 of (3)]. These human fossils belong to a minimum of six individuals.

Among the human fossils recovered in 1995 was a partial face, ATD6-69, of a juvenile individual assigned to hominid 3 (see Fig. 1 and Table 3). ATD6-69 shows a completely modern pattern of midfacial topography. In the modern human midface the infraorbital bone surface slopes down and slightly backward, producing a marked depressed area in the face (canine fossa). On the other hand, the coronal orientation of the infraorbital plate and the more sagittal one of the lateral nasal wall determines a maxillary flexion that can be seen in a transverse cross section. The inferior margin of the infraorbital plate (zygomaticoalveolar crest) is generally arched or even horizontal. ATD6-69 shares all these features with modern humans. The adult and more fragmentary specimen ATD6-58 also shows a maxillary depression, although it is much shallower. Both specimens and the adult ATD6-19

small fragment show a horizontal zygomaticoalveolar crest, with a high root. A vertical or anteroinferiorly sloping infraorbital surface is the primitive condition for hominids, as found in australopithecines, *H. habilis* s. l. (6) and *H. ergaster* (including KNM WT 15000, of roughly a similar age at death as hominid 3 from TD6). On the other hand, the nasal projection in these hominids is reduced (another primitive trait) and does not produce a marked maxillary flexion. In the Neandertal midface an infraorbital surface oriented halfway between coronally and sagittally continues in a flat bone surface (in some specimens it is even convex), until the nasal lateral margins (projected anteriorly). There is neither an infraorbital plate depression nor a maxillary flexion. The zygomaticoalveolar crest is straight and oblique in frontal view and has a low root.

No other specimens with the definitive modern midface characteristic of ATD6-69 have been found earlier than the first modern humans specimens of Djebel Irhoud 1, the Skhul and Qafzeh samples, and perhaps the Laetoli H18 specimen, although the older Dali and Florisbad fossils seem to approach this pattern. The adult TD specimen ATD6-58 shows that maxillary sinus expansion during adolescence tended to fill the maxillary hollowing, and this is probably why the modern facial morphology is not present in some adult middle Pleistocene ancestors of modern humans. The midfacial morphology of modern humans could be a retention of a juvenile pattern that was not yet present in *H. ergaster*, because WT 15000 displays the early *Homo* morphology. The derived Neandertal midface does not preserve, even in juvenile specimens, any traces of the ancestral morphology seen in the TD6 fossils, but transitional specimens like Atapuerca-Sima de los Huesos AT-404 and Steinheim indicate that the Neandertal pattern could have been derived from that of Gran Dolina.

The primitive *Homo* lacks a sharp, lower

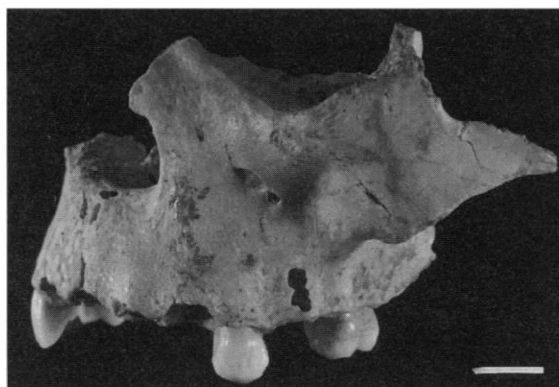


**Fig. 1.** ATD6-69 juvenile partial face. The fully modern facial topography is evident, including a prognathic (nonflat) midface, a well-developed canine fossa, a horizontal zygomaxillary border and a sharp lower nasal margin. The formation stage (CT-scan observation) and eruption of the teeth preserved in ATD6-69 suggest that the age at death was 10 to 11.5 years for this individual (20). Scale bar, 1 cm.

J. M. Bermúdez de Castro and A. Rosas, Museo Nacional de Ciencias Naturales, Consejo Superior de Investigaciones Científicas (CSIC), Departamento de Paleobiología, J. Gutiérrez Abascal 2, 28006 Madrid, Spain.

J. L. Arsuaga and I. Martínez, Departamento de Paleontología, Facultad de CC Geológicas, Instituto de Geología Económica UCM-CSIC, Unidad Asociada Atapuerca, Grupo de Paleoantropología, CSIC, Universidad Complutense de Madrid, 28040 Madrid, Spain.

E. Carbonell and M. Mosquera, Laboratori d'Arqueologia, Universitat Rovira i Virgili, Unidad Asociada Atapuerca, Grupo de Prehistoria, CSIC, Plaza Imperial Tàrraco 1, 43005 Tarragona, Spain.

\*To whom correspondence should be addressed.

nasal margin. Instead, a crest runs postero-laterally from the nasal spine across the nasal floor, and another crest extends from the lateral margin of the nasal aperture. Both crests are more clearly separated than in modern humans. All Pliocene to lower Pleistocene *Homo* fossils show this pattern (including the juvenile KNM WT 15000), as do middle Pleistocene fossils such as the Sima de los Huesos sample, Bodo, or Bro-

ken Hill. On the other hand Neandertals (including even young individuals) show a distinctive derived pattern of nasal crests, in which a solid bone projects medially into the nasal cavity (7). The Gran Dolina juvenile specimen ATD6-69 shows a fully modern pattern. The spinal crest and the lateral crest are close to each other and almost fused in an inferior nasal rim.

The data show that *H. antecessor* dis-

plays a unique combination of cranial, dental, and mandibular traits that collectively are different from that of other known *Homo* fossils. (Table 1). Most dental features are primitive for *Homo*, and

**Table 1.** Traits defining *Homo antecessor*.

Cranial traits	
1. Midfacial topography shows a fully modern pattern: infraorbital surface is coronally oriented and sloping downwards and backwards (true canine fossa), with a horizontal and high rooted inferior border.	
2. Supraorbital torus is doubled arched in frontal view.	
3. Superior border of the temporal squama is convex (arched).	
4. Presence of styloid process.	
5. Cranial capacity above 1000 cm <sup>3</sup> (14).	
Mandibular traits	
6. The mylohyoid groove extends anteriorly nearly horizontal and courses into the mandibular body as far as the level of the M2/M3 (15).	
7. Thickness of the mandibular body is clearly lesser than that of <i>H. ergaster</i> * and <i>H. habilis</i> s.s. (6), and specimens from Baringo, Java and OH 22.	
8. Absence of alveolar prominence at the M1 level.	
9. Extramolar sulcus is narrow.	
10. Lateral prominentia is smooth and restricted to the level of M2.	
11. Design of the inner aspect of the corpus defined by a shallow but well developed subalveolar fossa and a distinct internal oblique line, similar to that of European Middle Pleistocene fossils (16).	
Dental traits	
12. Mandibular incisors are buccolingually expanded with respect to <i>H. habilis</i> s. s., Zhoukoudian, and specimens such as KNM ER 992 and Dmanisi, although to a lesser degree than the <i>H. heidelbergensis</i> † and <i>H. neanderthalensis</i> .	
13. Postcanine teeth are smaller than those of <i>H. habilis</i> s. s., and within the range of <i>H. ergaster</i> , <i>H. erectus</i> ‡ and <i>H. heidelbergensis</i> .	
14. Maxillary incisors are shovel-shaped.	
15. Mandibular canine is mesiodistally short.	
16. Buccal faces of the lower premolars show mesial and distal marginal ridges and grooves, which connect with the shelf-like cingulum.	
17. Crown shape of the mandibular P3 is strongly asymmetrical.	
18. Mandibular P3 exhibits a remarkable talonid.	
19. P3 > P4 size sequence for the crown area of the upper and lower premolars.	
20. Upper and lower premolars are broad buccolingually.	
21. Mandibular M1 is buccolingually expanded with respect to <i>H. ergaster</i> .	
22. M1 < M2 size sequence for the crown area of the upper and lower molar series.	
23. Mandibular M3 is noticeably reduced with respect to the M1.	
24. Mandibular M1 and M2 show an Y-pattern of the buccal and lingual grooves separating the five principal cusps.	
25. Maxillary premolars show two, buccal and lingual, well separated roots.	
26. Mandibular P3 and P4 exhibit a complex root system, formed by a MB platelike root with two pulp canals and a DL root with a single canal (17).	
27. Roots of the mandibular and maxillary molars are well separated and divergent. These teeth present a moderate taurodontism (18).	
28. Root system of all teeth is short relative to the crown dimensions.	
29. Enamel of the occlusal surface of the postcanine teeth is moderate to remarkably crenulated.	

\*This taxon includes the following specimens: KNM ER 730, 820, 992, 3733, 3883 KNM WT 15000, and SK 847.

†This species includes only the European middle Pleistocene fossils. ‡In the Asian restricted sense.

**Table 2.** List of fossil hominid specimens recovered in 1995 and 1996 from TD6 (19). All inventory numbers (IN) are preceded by ATD6-. P, proximal; M, middle; D, distal; fg, fragment; L, left; R, right; Com., complete.

Specimen	IN
Shaft of a L rib	39
Diaphysis of a L radius	43
Subadult M manual phalanx. Com. bone	44
Spinous process of a lumbar vertebra	45
Crown of L LI2	48
Complete R adult clavicle	50
Complete 6th–7th cervical vertebra	51
Left LI1	52
M subadult manual phalanx. Com. bone	53
Partially complete subadult axis	54
Left subadult clavicle	55
Complete R adult patella	56
Most of a R temporal mastoid region, incl. posterior half of mastoid process	57
Left adult large zygomatic maxillary fg	58
Adult L metacarpal 2	59
Fg of frontal	61
Fg of mandibular corpus	63
Fg of a L rib. Neck and tubercle	66
Eroded P manual phalanx	67
D pedal phalanx. Com. adult bone	68
Partial face with R P3, M1, and germs of M2 and M3, and L I2-M1	69
Left adult metatarsal 2	70+107
Thoracic subadult vertebral body	74
Partially com. 3rd–4th cervical vertebra	75
P fg of a right femoral diaphysis	76
Right occipital condyle	77
Right 2nd rib	79
Fg of a thoracic vertebra	80
Basilar occipital/spheroid	81
P phalanx 2. Head of a left bone	82
Fg of zygomatic arch with the zygomaticotemporal suture	84
Shaft of a right rib	85
Vertebral end of a R rib	88
Complete adult atlas vertebra	90
Complete R 1st rib	108
Shaft of a L rib	206
Shaft of a R rib	251
Left UI2 germen	312

the mandibular anterior teeth are slightly enlarged with regards to early *Homo*, whereas the posterior teeth are reduced only at the M3 level. The corpus of the mandible lacks plesiomorphous *Homo* features, as well as those derived conditions developed during the middle Pleistocene. Finally, as discussed above, the midface of the TD6 hominids exhibits a completely modern pattern.

The TD6 hominids exhibit some derived craniofacial and dental traits, such as an arched superior border of the temporal squama, a forward location of the mylohyoid groove, absence of alveolar prominence, some expansion of the mandibular anterior teeth, and P3 > P4, all of them preserved in a primitive condition in *H. erectus*. In contrast, the differences in the position of the mylohy-

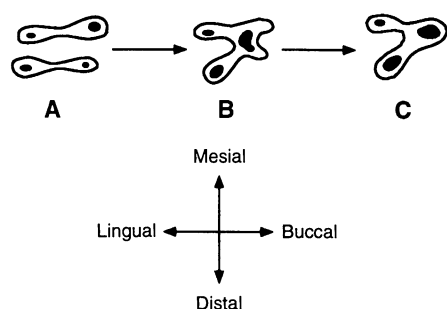


**Fig. 2.** Hypothetical transformation sequence from the primitive mandibular root form 2R: M + D (A) to the TD6 derived premolar root form (C). In the plesiomorphous condition, the buccal component of the mesial root is more developed than the lingual component. In contrast, the lingual component of the distal root is dominant. Both components of the mesial and distal roots have independent pulp canals. The most simple ontogenetic change to explain the transition from this primitive morphology to the form observed in the TD6 hominids would be the suppression of the DB interradicular process. This change would lead to the fusion of the buccal components of both the mesial and distal roots (B).

**Table 3.** Tooth measurements (in millimeters) of the hominids 3, 4, and 5 from TD6. M, mesiodistal; B, buccolingual. Teeth are maxillary teeth for hominid 3 and mandibular teeth for hominids 4 and 5.

Tooth	Side	M	B
<i>Hominid 3</i>			
I2	R	8.3	8.2
P3	R	8.8	11.5
P3	L	8.8	12.1
P4	R	—	11.6
M1	R	11.9	12.1
M1	L	12.0	12.0
<i>Hominid 4</i>			
I2	L	7.6	7.7
<i>Hominid 5</i>			
I1	L	—	7.6

oid groove, the geometry of the mandibular alveolar and basal borders, and the presence of the styloid process, which are preserved in their primitive condition in the TD6 hominids, indicate that there was a strong divergence between these hominids and *H. erectus* (8).

On the other hand, the reduced size of the mandibular M3 and canine indicates that the TD6 hominids have differed from *H. ergaster*. Furthermore, the TD6 mandible is gracile, as is indicated for instance by the absence of the alveolar prominence and the reduction of the thickness of the corpus. This feature also suggests that the TD6 hominids have differed from *H. ergaster*. The buccolingual enlargement of the mandibular M1, the elevation and arching of the temporal squama, the development of a more projected midface, the increase of the cranial capacity as well as the modern midface topography and subnasal morphology of the TD6 hominids, definitively separate them from this African species.

It has been suggested (2, 9, 10) that hominids such as Mauer, Vértesszöllos, Bilzingsleben, Arago, and Petralona, together with Bodo, Broken Hill 1, and Dali (among other middle Pleistocene fossils not considered to be *H. erectus*) form the stem group for Neandertals and modern humans and could be classified as a distinct species (*H. heidelbergensis*). However, the exclusive common ancestor of Neandertals and modern humans is not represented in the currently available European middle Pleistocene record. We suggest that all the European middle Pleistocene fossils are ancestors (only) of the late Pleistocene Neandertals (3, 11). Moreover, the holotype, the Mauer mandible, shows clear derived neandertal traits, such as a large retromolar space, whereas teeth shape and morphology are indistinguishable from those of Neandertals (12). The species *H. heidelbergensis* is thus only acceptable in a restricted sense as a European chronospecies directly ancestor to Neandertals.

Several authors (13) have suggested that *H. erectus* was ancestral neither to modern humans nor to Neandertals but was a separate lineage that went extinct without descendants. In agreement with this notion, the TD6 sample shows two primitive features (presence of styloid process and doubled arched supraorbital torus) in which *H. erectus* manifests the derived condition. The TD6 hominids also display a set of primitive dental traits shared only with *H. ergaster* and *H. erectus*, such as the presence of cingulum in mandibular canine and premolars, an asymmetry of the crown of the mandibular P3, and a well-developed talonid in the mandibular P3. On the other hand, the TD6 hominids exhibit some derived traits not

present in *H. erectus* and *H. ergaster*, namely, a high and convex superior border of the temporal squama, a gracile mandibular corpus with no alveolar prominence, a noticeable brain expansion, and a fully modern midface topography. This is the most suitable combination of traits from which the modern human and neandertal morphology could be derived. Thus, we suggest that Neandertals derived their peculiar midfacial and mandibular specializations from *H. antecessor* through the European middle Pleistocene populations (for example, Mauer, Petralona, Arago, Steinheim, and the Sima de los Huesos samples).

Finally, the root system of the mandibular premolars of hominid 1 from TD6 represents one primitive expression of a hominid morphological polymorphism (Fig. 2). This particular root morphology suggests that there is a relation between the TD6 hominids and certain East African lower Pleistocene populations. Furthermore, the BL expansion of the mandibular anterior teeth and the mylohyoid line position, which are shared by *H. antecessor* and some late *H. ergaster* specimens, point to a closer phylogenetic relation between both species.

## REFERENCES AND NOTES

1. M. H. Wolpoff, *Paleo-Anthropology* (Knopf, New York, 1980), chap 10.
2. G. P. Rightmire, *J. Hum. Evol.* **31**, 21 (1996).
3. E. Carbonell et al., *Science* **269**, 826 (1995).
4. J. M. Parés and A. Pérez-González, *ibid.*, p. 830.
5. *Etymology*. The name *antecessor* is the Latin word meaning explorer, pioneer, early settler. Assigning this name we emphasize that the TD6 hominids belong to the first population as yet known in the European continent. *Types*. The holotype is a fragment of right mandibular body with M1, M2, and M3 (ATD6-5) and an associated set of teeth from the same individual that includes: right P3, P4, M1, and M2, left C, P3, P4, and M1; lower right C (crown fragment) P3, and P4, and left I2. Found by the Atapuerca research team in July 1994. The fossil remains of the holotype and paratypes found in 1994 are listed in table 1 of (3). Most of the remains of the holotype are shown in figure 3 of (3). The paratypes found in 1995 and 1996 are listed in Table 2. Holotype and paratypes are provisionally housed in the Museo Nacional de Ciencias Naturales de Madrid, CSIC, Spain. The final repository of the fossils is the Museo de Burgos. *Locality*. The Sierra de Atapuerca is situated about 0°10'E and 42°20'N. It is near the Arlanzón River and is 14 km east from the city of Burgos, northern Spain. All the fossil specimens attributed to the new species come from the Gran Dolina site (TD). The TD site is 18 m deep and fills the cavity catalogued as BU-IV-A-16 [M. A. Martín, S. Domingo, T. Antón, *Kaite* **2**, 41 (1981)]. This cavity is located in the Trinchera del Ferrocarril, a dismantled railway trench opened in the southwestern side of the Sierra de Atapuerca. *Horizon*. All the types come from the so-called Aurora stratum, one of the Lower Pleistocene strata of the TD6 level. The top of the Aurora stratum is about 1 m below the Matuyama-Brunhes boundary (4).
6. According to B. A. Wood, *Nature* **355**, 783 (1992).
7. J. H. Schwartz, and I. Tattersall, *Proc. Natl. Acad. Sci. U.S.A.* **93**, 10,852 (1996).
8. The reported Ceprano fossil from Italy, perhaps of early middle Pleistocene or even lower Pleistocene age, has been described as a late *H. erectus* [A.

- Ascenzi, I. Biddittu, P. F. Cassoli, A. G. Segre, E. Segre-Naldini, *J. Hum. Evol.* **31**, 409 (1996)], which if confirmed (both the date and the taxonomic assignment) would represent the coexistence of two different hominid species in Europe.
9. C. B. Stringer, *ibid.* **12**, 731 (1983); C. B. Stringer, in *Ancestors: The Hard Evidence*, E. Delson, Ed. (Liss, New York, 1985), pp. 289–295; C. B. Stringer, in *Aux Origines des Homo sapiens*, J. J. Hublin and A. M. Tiller, Eds. (Presses Universitaires de France, Paris, 1991), pp. 49–74.
  10. I. Tattersall, *The Last Neanderthal* (Macmillan, New York, 1986).
  11. A. Rosas, J. M. Bermúdez de Castro, E. Aguirre, *L'Anthropologie* **95**, 89 (1991); J. L. Arsuaga, I. Martínez, A. Gracia, J. M. Carretero, E. Carbonell, *Nature* **362**, 534 (1993); J. L. Arsuaga et al., *Rev. Esp. Paleontol.* **nº Extraord.**, 269 (1996); J. L. Arsuaga, I. Martínez, A. Gracia, C. Lorenzo, *J. Hum. Evol.*, in press.
  12. A. Rosas and A. Buscalioni, *Rev. Esp. Paleontol.* **12**, 23 (1997); A. Rosas, in *Atapuerca y Evolución Humana*, E. Aguirre, Ed. (Fundación Ramón Areces, Madrid, in press); J. M. Bermúdez de Castro, M. E. Nicolás, J. Rodríguez, in *ibid.*
  13. P. Andrews, in *The Early Evolution of Man with Special Emphasis on Southeast Asia and Africa*, P. Andrews and J. L. Franzen Eds. (Courier Forsch.-Inst. Senckenberg: Frankfurt a. M., 1984), pp. 167–175; C. B. Stringer, in *ibid.*, pp. 131–143; B. A. Wood, in *ibid.*, pp. 99–111.
  14. ATD6-15 minimum frontal breadth and bitemporal breadth is 95 to 100 mm and 100 mm, respectively. These sizes are well above those of ER 3733, ER 3883, Sangiran 2, or Trinil (all skulls with cranial capacities below 1000 cm<sup>3</sup>). In spite of its thin frontal squama and delicate supraorbital torus, ATD6-15 was initially considered to be an adolescent because of its extensive frontal sinuses (3); however, because WT 15000 also shows a well-developed frontal sinus, ATD6-15 could well have belonged to an individual of similar age at death (around 11 years old), maybe the same individual as the ATD6-69 face.
  15. The myelohyoid groove maintains with the alveolar margin a fairly low angle of about 34°. The only other fossil *Homo* mandible that approximates the form of the ATD6-5 myelohyoid groove is that of WT-15000. In the European middle Pleistocene hominids and Neandertals, the groove lies farther behind M3, and has an angle of 52° to 57° (mean of 12 is 54.9°).
  16. A. Rosas, *J. Hum. Evol.* **28**, 533 (1995).
  17. This morphology probably derives from the presumed primitive condition 2R: M + D of the ape-hominid clade, which characterizes some early Pleistocene hominids from the Koobi Fora region [B. A. Wood, S. A. Abbott, H. Uytterschaut, *J. Anat.* **156**, 107 (1988)].
  18. The molars from TD6 are included in the category of hypotaurodontism [J. C. Shaw, *J. Anat.* **62**, 476 (1928)]. The trend to the total fusion of the roots leads to the meso and hypertaurodontism which seems to be a derived condition of *H. heidelbergensis* and *H. neanderthalensis*.
  19. The identification of the postcranial remains was made by J. M. Carretero, A. Gracia, and C. Lorenzo.
  20. Age at death was estimated using values for predicting age from stages of permanent tooth formation presented in tables 9 and 10 of B. H. Smith [in *Advances in Dental Anthropology*, M. A. Kelley and C. S. Larsen Eds. (Wiley-Liss, New York, 1991), pp. 143–168].
  21. We dedicate this paper to Emiliano Aguirre, pioneer of the systematic excavations and research in the Sierra de Atapuerca. The excavations in the Sierra de Atapuerca are supported by the Junta de Castilla y León, and the Research Project by the Ministerio de Educación y Cultura (DGLCYT, project no. PB93-0066-C03, and Unidad Asociada Atapuerca). We thank the Atapuerca research team. Special thanks are given to those who have excavated the Aurora stratum from TD6. We are also grateful to I. Tattersall, J. Schwartz, J. Rodríguez, E. Nicolás, J. van der Made, and three anonymous reviewers for comments on the manuscript. The human fossils were restored by P. Gutiérrez del Solar and B. Gómez-Alonso.

6 February 1997; accepted 15 April 1997

## Tin-Based Amorphous Oxide: A High-Capacity Lithium-Ion-Storage Material

Yoshio Idota, Tadahiko Kubota, Akihiro Matsufuji,  
Yukio Maekawa, Tsutomu Miyasaka\*

A high-capacity lithium-storage material in metal-oxide form has been synthesized that can replace the carbon-based lithium intercalation materials currently in extensive use as the negative electrode (anode) of lithium-ion rechargeable batteries. This tin-based amorphous composite oxide (TCO) contains Sn(II)-O as the active center for lithium insertion and other glass-forming elements, which make up an oxide network. The TCO anode yields a specific capacity for reversible lithium adsorption more than 50 percent higher than those of the carbon families that persists after charge-discharge cycling when coupled with a lithium cobalt oxide cathode. Lithium-7 nuclear magnetic resonance measurements evidenced the high ionic state of lithium retained in the charged state, in which TCO accepted 8 moles of lithium ions per unit mole.

Lithium-ion insertion materials have gained considerable attention because they can be used as an active electrode in Li-ion rechargeable batteries, which have potential applications ranging from portable electronic devices to electric vehicles. Until 1980, Li metals and alloys were used as anode (negative electrode) materials in combination with various solid-solution cathode materials (1) in Li-ion batteries. From 1985 onward, the sole alternative to the Li metal anode, adopted to overcome safety problems, were carbon-based Li-ion intercalation materials (2), which intro-

duced the concept of a "rocking-chair" type of rechargeable battery. Lithium ions are reversibly stored between layered carbon frameworks, which thereby develop an electrochemical potential relative to the Li/Li<sup>+</sup> anode low enough to act as negative electrodes. There have been important improvements in the Li-storage capacity of carbon materials that allow it to exceed the stoichiometric limit of Li-ion intercalation in graphite (LiC<sub>6</sub>), 372 milliampere-hours per gram (mA·hour/g) of C<sub>6</sub> (3). The possibility of creating high-capacity anodes that leapfrog this limit has been demonstrated with the deep doping of Li (4, 5). A significant trade off occurs, however, with regard to the ability to guarantee the safety of high-capacity anodes after repeated charge-discharge operations, which often cause the formation of

hazardous metallic Li (dendrite) on the electrode surface (6).

We have synthesized an amorphous metal-oxide material that can store Li ions with a Coulombic capacity reaching that of hydrogen-storage alloys, ensuring protection against dendritic Li formation. The amorphous material is a metal composite oxide glass that contains tin(II) oxide as an active center for Li adsorption. It provides a gravimetric capacity of >600 mA·hour/g (0.022 mol of Li per gram) for reversible Li adsorption and release, which corresponds in terms of reversible capacity per unit volume to more than 2200 mA·hour/cm<sup>3</sup> (0.075 mol of Li per cubic centimeter). The latter value is about twice the reversible capacity of state-of-the-art high-capacity carbon materials (840 to 1200 mA·hour/cm<sup>3</sup>) (5).

The tin-based composite oxide (TCO) active material has a basic formula represented by SnM<sub>x</sub>O<sub>y</sub>, where M is a group of glass-forming metallic elements whose total stoichiometric number is equal to or more than that of tin ( $x \geq 1$ ) and is typically comprised of a mixture of B(III), P(V), and Al(III). In the oxide structure, Sn(II) forms the electrochemically active center for Li insertion and potential development, and the other metal group provides an electrochemically inactive network of (M–O)– bonding that delocalizes the Sn(II) active center. To confer high reversibility in Li storage and release, the Sn–O framework was thus anisotropically expanded by incorporating glass-forming network elements—B, P, and Al—in view of the enhancement of Li-ion mobility in the anisotropic glass structure, favorable

Y. Idota and T. Kubota, Fujifilm Celltec, Matsuzakadaira 1–6, Taiwa-cho, Kurokawa-gun, Miyagi 981–34, Japan. A. Matsufuji, Y. Maekawa, T. Miyasaka, Ashigara Research Laboratories, Fuji Photo Film, Nakanuma 210, Minamiashigara, Kanagawa 250–01, Japan.

\*To whom correspondence should be addressed.